SLAC–PUB–6624
Aug 1994
(A)

Contributed to the 17th International Linac Conference, Tsukuba, Japan, Aug 21–26, 1994

HIGHER ORDER MODE DAMPING FOR A DETUNED STRUCTURE*

N. Kroll†, K. Thompson, K. Bane, R. Gluckstern‡, K. Ko, R. Miller, and R. Ruth

Stanford Linear Accelerator Center, Stanford University, Stanford, CA 94309 USA

† Physics Department, University of California, San Diego, La Jolla, CA 92093

‡ Physics Department, University of Maryland, College Park, MA 20742

INTRODUCTION

The acceleration cavities [1] for the NLC test accelerator (NLCTA) are disk-loaded structures composed of 204 cells plus two couplers, 1.8 meters in length, and driven at 11.424 GHz. In order to suppress the transverse wakefield the structures are detuned [2]. As a result, the widths of the higher order mode (HOM) bands are increased, and the cell-to-cell amplitude variation of the individual modes in a band is drastically altered. Thus an off-center charge bunch moving at the velocity of light excites a spread of modes per band rather than the single (synchronous) mode characteristic of a strictly periodic structure, and the average deflecting force experienced by a charge at fixed trailing distance s falls off sharply in s at a rate proportional to the frequency spread of the excitation within the band. The predicted behavior of this wakefield is shown in Fig. 22 of Ref. 1. While the wakefield does exhibit an initial rapid fall off, it reappears after a few meters [4]. This effect is associated with the fact that the mode distribution within a band is discrete rather than continuous, and as the elapsed time begins to exceed the inverse mode separation the suppressing effect of a smooth gaussian distribution is lost. As discussed in Ref. 1, this reappearance can be postponed by interleaving the detuning among four such structures so as to lead to a factor four increase in the effective mode spectrum density. However, submicron tolerances are needed to achieve this extended suppression.

We report in this paper the current status of our investigation of the possibility of suppressing the wake reappearance by providing relatively weak damping via the vacuum manifolds. Our proposed structure is illustrated in Fig. 1. The four vacuum manifolds running the length of the structure also function as multimode waveguides which serve to drain power from the HOM's through the large coupling slots located in each cell, except, as discussed later, for a few at each end of the manifolds.

The waveguides are designed so that the acceleration mode is undamped, but there is still some limit on the size of the coupling slots because of their effect on its shunt impedance. We have set a limit of 5% degradation as a working figure, which limits the space occupied by the slots to approximately one third of the cell circumference. The effectiveness of the manifolds as dampers for the HOM's is connected to the detuning in an essential way. The HOM's of the detuned structure are localized standing waves with spatial variation of effective wavelength which varies smoothly and extensively along the length of the mode. This is precisely the feature which allows many modes in a band to be excited by a velocity of light particle. The excitation pattern of the mode as seen by the waveguide is such that it can drive a manifold wave at a broad range of phase velocities. The coupling of a cavity mode to the manifold is strongest when this range of phase velocities overlaps the phase velocity of one or more manifold modes at the frequency of the cavity mode.

⋆ Work supported by Department of Energy contracts DE–AC03–76SF00515 and DE-FG03-93ER40759.

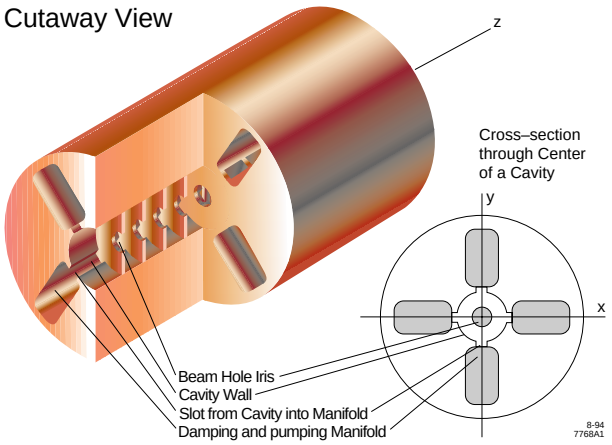

Figure 1. The damped detuned structure.

MANIFOLD AND DETUNED DIPOLE MODES

From Fig. 1 we see that the damping waveguides are approximately rectangular in cross section, and consequently their modes can be designated by rectangular waveguide notation. The cutoff frequencies of the set of potentially relevant modes are listed in Table 1.

Table 1: Manifold modes and their cutoffs in GHz

TE_{10}	TE_{01}	TE_{20}	TM_{11}	TE_{11}	TM_{21}
6.042	11.507	11.926	12.645	13.464	16.076

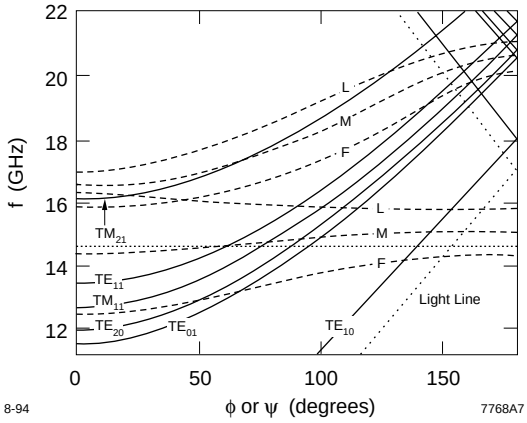

Figure 2. Dispersion curves for the manifold modes designated in Table 1 overlaying dispersion curves for the first two dipole modes of the first (F), middle (M), and last (L) cells. A cavity mode line (·····) is also shown.

The frequencies of these modes as a function of phase advance per period are shown in Fig. 2. We see that the only mode which is propagating at 11.424 GHz is the TE_{10}, which cannot couple to the accelerating mode because of symmetry mismatch. Fig. 2 also shows dispersion curves of the first two dipole modes for three cells of the detuned structure. It is apparent that the dispersion curve for each cell crosses the dispersion curve of several manifold modes.

To qualitatively explain the damping process we consider a single cavity mode, represented in Fig. 2 by a horizontal line at its frequency. This particular mode is localized because its mode line extends over the full phase range without intersecting the first or last cell, the excited cells being those whose dispersion curves intersect the mode line. The point where the light line intersects the mode line lies on some cell dispersion curve (or between two of them), which tells us where in the structure the mode couples effectively to the drive bunch. Similarly, the intersections of the manifold mode dispersion curves with the mode line determine the localized regions where effective coupling to the crossing mode occurs. Modes whose lines intersect the first or last cell terminate there and, correspondingly, extend to one or both ends of the structure. It is easy to see that every cavity mode line of the lower band which crosses the light line must also cross the dispersion curve of every propagating manifold mode. Also, the upper dipole mode has cavity mode lines which terminate on the first and last cell and are therefore not localized. There are fewer manifold mode crossings, but there do not appear to be any cases for which a cavity mode which crosses the light line has less than two manifold mode crossings.

EQUIVALENT CIRCUIT MODEL

The quantitative results that we report in this paper have all been obtained with a simplified equivalent circuit model. Following [3] we start with a single circuit chain in which each circuit corresponds to a single cell mode and the cells are coupled magnetically. We describe the manifold modes as transmission lines and use standard transmission line equations with the series reactance per unit length X and shunt susceptence per unit length B modified so as to produce the proper waveguide propagation behavior and a characteristic impedence with the proper frequency dependence. We model the coupling between each cell and the manifold mode via a mutual inductance between the cell inductance and one of a periodic set of lumped series inductances in the transmission line localized at each coupling slot. This model leads to a set of coupled equations:

$$\begin{aligned}&(\frac{1}{f_m^2}-\frac{1}{f^2})a_m+\frac{k_{m+\frac{1}{2}}}{2}a_{m+1}+\frac{k_{m-\frac{1}{2}}}{2}a_{m-1}\\&-j\phi\frac{k}{k_g}\frac{Z_0}{Z}\sum_n \hat{k}_m\hat{k}_n\exp(-j\phi|n-m|)a_n=0\quad ,\end{aligned}\tag{1}$$

Here the notation for the cell amplitude coefficients a_m, the cell frequencies f_m, and the cell to cell coupling coefficients $k_{m+\frac{1}{2}}$ follows [1] section 3.3.1. The $\hat{k}_m$ represent the coupling between the manifold and cell m. For the present we take $\phi = k_g P$ where P is the structure period, and $Z_0/Z = k_g/k$ (TE mode) or $Z_0/Z = k/k_g$ (TM mode). These specifications would be somewhat modified if we were to take account of the effect of the lumped series inductances on the transmission line properties. The last term of Eq. (1) (i.e., the summation term) represents coupling to a single manifold mode. To represent the actual situation it should include a similar sum over all propagating modes, with appropriate modifications to represent different manifold mode types. However, the model calculations to be discussed in this paper will be limited to a single mode.

APPLICATIONS OF THE MODEL

We have studied the implications of Eq. (1) for a single set of parameters for the undamped problem. These were selected to correspond to a simplified version of the NLC test accelerator cavity, following the procedure specified in Ref. 3. To simplify the exploration of the dependence upon the manifold coupling parameters we limit parameter variation in the damping matrix to the manifold cutoff frequency f_c (always taken below the frequency of the cavity modes) and to an overall scale factor for the $\hat{k}_m$. The specific form taken was

$$\hat{k}_m = \hat{\eta}/f_m \quad , \tag{2}$$

where $\hat{\eta}$ is the dimensionless scale factor, and the factor $1/f_m$ is inserted to obtain the correct dimensions. We set $\hat{k}_m$ equal to zero for the last six cells on each end so as to make it possible to insert the absorbers into the manifold ends without extending them beyond the length of the cavity. The mode frequencies and amplitude distributions of Eq. (1) cannot be found by the standard matrix diagonalization methods because the damping matrix involves the frequency in a complicated way. The (complex) frequencies were instead determined by an iterative procedure and Q is defined as usual as $\mathrm{Re}(f)/2\mathrm{Im}(f)$.

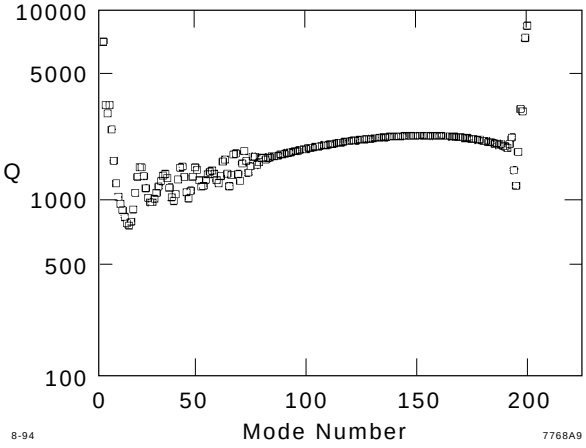

Figure 3. Damping by a single manifold mode computed for the single band model. Manifold mode cutoff = 12 GHz and manifold coupling parameter $\hat{\eta} = 0.0106$.

Figure 3 is a plot of the Q values of these modes as a function of mode number (numbered from lowest to highest frequency), for f_c of 12 GHz and $\hat{\eta} = 0.0106$. The scatter in the perturbed frequencies (i.e., the real part) of the modes is of order a part in 10^4. Both frequency and Q distributions become smoother as $\hat{\eta}$ is decreased with the overall magnitude varying roughly as $\hat{\eta}^2$. We note that Q's of the order of 1000 correspond to a resonance width, f/Q, twice as large as the mode separation at the peak of the mode spectrum. Thus, as the coupling is made stronger, substantial distortion of the mode patterns is expected, and because the group of cells within the mode which are well coupled to the manifold mode is localized, there is a tendency of the modes to split into more weakly and more strongly damped groups. We have also varied f_c from zero to 12 GHz. We find that those modes whose mode lines cut the light line are damped about as well as those shown in Fig. 3, but there are more very weakly damped modes at

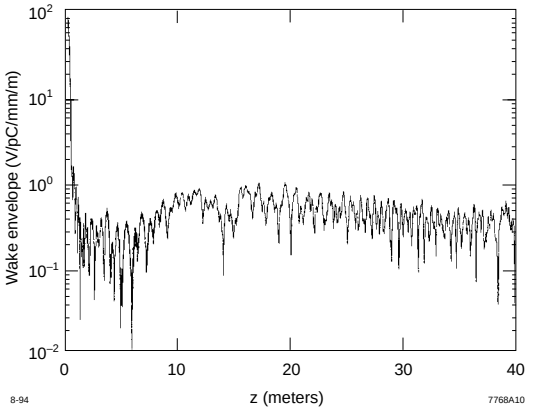

Figure 4. Wakefield for the parameters used for Fig 3. The effect of copper losses have been included by combining the Q values of Fig. 3 with an assumed copper loss value of 6500.

the low frequency end associated with the fact that their mode lines do not cut the manifold mode dispersion curve.

Figure 4 shows the wakefield computed for the Fig. 3 parameters using the Q values and perturbed frequencies with the kick factors of the undamped modes. It would be straightforward to obtain the perturbed amplitude distribution functions and to calculate the wakefield from them, but this calculation has not yet been carried out. Comparing to Fig. 22 of Ref. 1, we see that the reappearance at large distances has been largely suppressed. The deep minimum shown in that figure has also disappeared, an effect believed to be due to the scatter in the perturbed frequencies. If the coupling is made too large, this scatter and the resulting wakefield at a few meters become unacceptably large. Thus there is an optimum intermediate range of couplings.

MANIFOLD COUPLING PARAMETERS

In order to relate the manifold coupling parameter $\hat{\eta}$ to a physical structure, we have used MAFIA to study the spectrum of single cells coupled to the manifolds as a function of phase advance. Since this represents a periodic structure, we specialize Eq. (1) to this case. Thus we set $f_m = F$, $k_m = K$, and $a_m = A\exp(j\psi m)$. The sum may then be carried out and in the TE case results in

$$(\frac{1}{F^2} - \frac{1}{f^2} + K\cos\psi)(\cos\psi - \cos\phi) = \hat{\eta}^2\phi\frac{\sin\phi}{F^2}. \qquad (3)$$

Eq. (3) exhibits typical avoided crossing behavior around the (ψ, f) pair where both factors on the LHS vanish. The detailed form of the curves in the vicinity of the avoided crossing is very sensitive to the value of $\hat{\eta}$.

Figure 5 is obtained from a series of MAFIA runs for a single structure but for varying phase advance. Several avoided crossings are evident, associated with different manifold modes. We assume the crossings can be treated as though well separated from each other, and that the immediate vicinity of each crossing can be fit with Eq. (3). For our current preliminary assessment we have applied (3) to all of the crossings, regardless of the type of the manifold mode. The results of this procedure are shown on Fig. 5. We have carried out such an analysis for four different cell designs intended to approximate the current detuned structure design. The beam iris design corresponds precisely to particular cells. The coupling slots are taken to

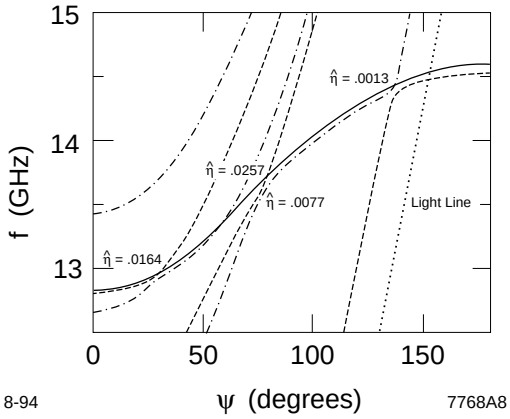

Figure 5. MAFIA computed mode frequencies for cell 10 of the detuned structure coupled to four manifolds with a set of phase advances per period specified. The frequency range shown restricts the figure to the lower dipole mode and to the avoided crossing manifold modes. The shunt impedence degradation of the accelerating mode is 2%; coupling constants $\hat{\eta}$ computed for each avoided crossing are shown on the figure. The solid curve represents undamped dipole mode.

be of uniform width and thickness and with length equal to the distance between beam irises. Because of the coupling slots the cell radius has to be reduced so as to maintain the proper phase advance for the accelerating mode. The values of effective coupling vary with the cell, but $\hat{\eta} = 0.0106$ used in Figs. 3 and 4 is quite easy to obtain in the proposed geometry. Furthermore the average degradation of the shunt impedence for the four cells is 2.3%, consistent with our working limit.

FUTURE PLANS AND CONCLUDING REMARKS

While the theory presented above is quite crude, it does allow us to hope that an effective damped detuned structure can be designed along these lines. Some obvious theoretical improvements are planned or in progress. An experimental program involving a full scale version of such a structure is being planned. The presence of the manifolds enhances cold test opportunities. Because of the localization of the important detuned modes within the structure it has not been possible to observe them directly with cold test procedures. The manifolds provide access to all of them, and it should be possible to demonstrate HOM damping via RF transmission from one manifold to another through the cavity cells. Direct observation of the wakefield as in [4] is of course also planned. Observation of the frequency spectrum of the beam induced radiation out of the manifold will also provide valuable beam diagnostic information.

We thank the other members of the structures group for useful discussions and comments.

REFERENCES

[1] K. Thompson, et al, SLAC-PUB-6032, November 1993, and references therein. To appear in Particle Accelerators.

[2] The cell dimensions are varied so as to obtain a gaussian distribution of dipole mode frequencies.

[3] Karl L.F. Bane and Robert L. Gluckstern, Part. Accel. **42**, 123 (1993); SLAC-PUB-5783.

[4] The wakefield of an accelerator cavity built as specified in [1] has recently been measured and found to be in reasonable agreement with Fig. 22 of Ref. 1, although the reappearance effect is somewhat less than expected. See C. Adolphsen, et al. TN-52 this conference.